Reduced-Order Robust Superdirective Beamforming With Uniform Linear Microphone Arrays

Chao Pan, Jingdong Chen, *Senior Member, IEEE*, and Jacob Benesty

***Abstract*—Sensor arrays for audio and speech signal acquisition are generally required to have frequency-invariant beampatterns to avoid adding spectral distortion to the broadband signals of interest. One way to obtain frequency-invariant beampatterns is via superdirective beamforming. However, traditional superdirective beamformers may cause significant white noise amplification (particularly at low frequencies), making them sensitive to uncorrelated white noise. To circumvent the problem of white noise amplification, a method was developed to find the superdirective beamforming filter with a constraint on the white noise gain (WNG), leading to the so-called WNG-constrained superdirective beamformer. But this method damages the frequency invariance of the beampattern. In this paper, we develop a flatness-constrained robust superdirective beamformer. We divide the overall beamformer into two subbeamformers, which are convolved together: one subbeamformer forms a lower order superdirective beampattern while the other attempts to improve the WNG. We show that this robust approach can improve the WNG while limiting the frequency dependency of the beampattern at the same time.**

***Index Terms*—Beampattern design, cardioid, directivity factor, microphone arrays, robust beamforming, superdirective beamforming, white noise gain.**

I. Introduction

MICROPHONE arrays combined with beamforming algorithms are often used to acquire audio signals of interest from noisy environments. The basic idea of beamforming is to form a spatial response with its main lobe pointing to a desired look direction to pick up the signal of interest while attenuating noise and interference from other directions. Since audio and speech signals are broadband in nature, microphone arrays are generally required to have frequency-invariant beampatterns to avoid adding artifacts to both the signal of interest and background noise [1]. Many algorithms have been developed to deal with the problem of frequency-invariant beamforming over the last two decades, such as differential microphone arrays (DMAs) [2]–[10], constant beamwidth beamforming [11]–[15], and eigenbeamforming [16]–[20]. In this paper, we focus on superdirective beamforming with uniform linear arrays (ULAs). The major reasons that we choose superdirective beamforming are as follows. First, this beamformer is derived from the maximization of the directivity factor (DF) (which is defined as the ratio between the magnitude squared beampattern in the look direction and the averaged magnitude squared beampattern over the entire space); consequently, it is more efficient than many other beamformers in dealing with signal acquisition in reverberant room acoustic environments where reflections are numerous, which form a diffuse noise field. Second, it can form frequency-invariant beampatterns when the interelement spacing is smaller than the minimum wavelength of the interested frequency range and, therefore, is good for processing broadband signals like speech [1], [33].

However, one major issue with superdirective beamforming is that it may cause significant white noise amplification (particularly at low frequencies), making it sensitive to sensor self noise. Much effort has been devoted to this problem and the solutions developed so far can be categorized into four classes. The first one is to apply a constraint on the white noise gain (WNG) while maximizing the DF, leading to the so-called WNG-constrained superdirective beamformer [21]–[23]. The second one is through properly combining the maximum WNG and maximum DF beamformers [24]. The third class is to implement the superdirective beamformer in a multistage way as the approach in [25]. And the last one is through jointly optimizing the DF, frequency-invariant beampattern, and WNG [26]. While they all can help improve the WNG, the first three classes generally make the beampattern frequency dependent and the last one does not have much flexibility in controlling the DF.

This paper also deals with superdirective beamforming with ULAs. We divide the overall beamformer into two sub-beamformers, which are convolved together: one sub-beamformer forms a lower-order superdirective beampattern while the other attempts to improve the WNG. Compared with the traditional approaches in [21]–[25], the proposed reduced-order superdirective beamformer can form frequency-invariant beampatterns while in comparison with the joint-optimization approach in [26], the DF of the proposed approach can be easily controlled. Moreover, the proposed approach can be used to design robust versions of other frequency-invariant beamformers.

The organization of this paper is as follows. In Section II, we present the signal model, performance measures, and problem formulation. In Section III, we present the beamformer

Manuscript received December 11, 2015; revised April 04, 2016; accepted May 09, 2016. Date of publication May 12, 2016; date of current version June 21, 2016. This work was supported in part by the National Natural Science Foundation of China “Distinguished Young Scientists Fund” under Grant 61425005. The work of C. Pan was supported by the China Scholarship Council, Innovation Foundation for Doctor Dissertation of Northwestern Polytechnical University, and Excellent Doctorate Foundation of Northwestern Polytechnical University. The associate editor coordinating the review of this manuscript and approving it for publication was Dr. Richard Hendriks.

C. Pan is with the Center of Intelligent Acoustics and Immersive Communications, School of Marine Science and Technology, Northwestern Polytechnical University, Xi’an 710072, China, and also with the INRS-EMT, University of Quebec, Montreal, QC H5A 1K6, Canada (e-mail: panchao2nwpu@mail.nwpu.edu.cn).

J. Chen is with the Center of Intelligent Acoustics and Immersive Communications, Northwestern Polytechnical University, Xi’an 710072, China (e-mail: jingdongchen@ieee.org).

J. Benesty is with INRS-EMT, University of Quebec, Montreal, QC H5A 1K6, Canada (e-mail: benesty@emt.inrs.ca).

Color versions of one or more of the figures in this paper are available online at http://ieeexplore.ieee.org.

Digital Object Identifier 10.1109/TASLP.2016.2568044

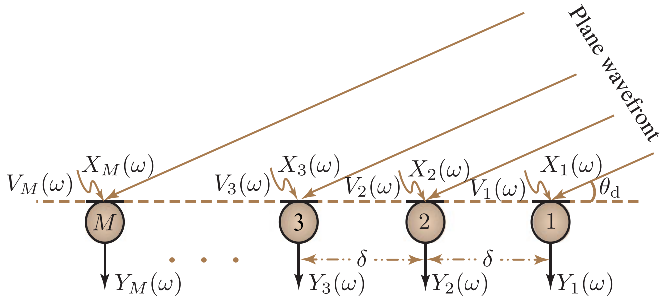

Fig. 1. Illustration of a uniform linear array system in the frequency domain.

structure and develop a flatness-constrained beamformer along with the maximum flatness and maximum WNG beamformers. In Section IV, we assess the flatness-constrained beamformer by means of beampattern, DF, and WNG. We then discuss how to extend the principle of flatness-constrained beamforming to the design of the cardioid beampattern in Section V. Finally, our conclusions are given in Section VI.

II. Signal Model, Performance Measures, and Problem Formulation

A. Signal Model in the Frequency Domain

We consider a far-field desired source signal that propagates in an anechoic acoustic environment and impinges on an M-element ULA from the $\theta_{\rm d}$ direction, as shown in Fig. 1. The observation of the mth ($m = 1, 2, \ldots, M$) microphone in the frequency domain can be written as [2]

$$\begin{aligned} Y_m(\omega) &= X_m(\omega) + V_m(\omega) \\ &= e^{-\jmath(m-1)\omega\tau_0 \cos\theta_{\rm d}} X(\omega) + V_m(\omega), \end{aligned} \tag{1}$$

where the zero-mean signals $X_m(\omega)$ and $V_m(\omega)$ are the desired and noise signals at the mth microphone, respectively, which are assumed to be uncorrelated, $X(\omega)$ is the source signal at the first sensor, $\omega = 2\pi f$ is the angular frequency with f being the temporal frequency, $\tau_0 = \delta/c$, δ is the interelement spacing, and $c = 340$ m/s is the speed of sound in the air.

Putting all the M microphone signals together into a vector form, we can rewrite the signal model in (1) as

$$\begin{aligned} \mathbf{y}(\omega) &\triangleq \begin{bmatrix} Y_1(\omega) & Y_2(\omega) & \ldots & Y_M(\omega) \end{bmatrix}^T \\ &= \mathbf{d}_M(\omega, \cos\theta_{\rm d}) X(\omega) + \mathbf{v}(\omega), \end{aligned} \tag{2}$$

where the superscript ^{T} is the transpose operator

$$\begin{aligned} &\mathbf{d}_M(\omega, \cos\theta_{\rm d}) \\ &\triangleq \begin{bmatrix} 1 & e^{-\jmath\omega\tau_0\cos\theta_{\rm d}} & \ldots & e^{-\jmath(M-1)\omega\tau_0\cos\theta_{\rm d}} \end{bmatrix}^T \end{aligned} \tag{3}$$

is a phase-delay vector of length M (whose form is the same as the steering vector used in traditional beamforming) that characterizes the signal propagation, and $\mathbf{v}(\omega)$ is the noise vector defined in a similar way to $\mathbf{y}(\omega)$.

Beamforming is a process that applies a linear filter, $\mathbf{h}(\omega) = [H_1(\omega)\ H_2(\omega)\ \ldots\ H_M(\omega)]^T$, to the observation vector, $\mathbf{y}(\omega)$, thereby obtaining an estimate of the source signal, $X(\omega)$, i.e., [28]

$$\begin{aligned} \chi(\omega) &= \mathbf{h}^H(\omega)\mathbf{y}(\omega) \\ &= \mathbf{h}^H(\omega)\mathbf{d}_M(\omega, \cos\theta_{\rm d})X(\omega) + \mathbf{h}^H(\omega)\mathbf{v}(\omega), \end{aligned} \tag{4}$$

where the superscript ^{H} is the conjugate-transpose operator. The objective of fixed beamforming is to find an optimal filter, $\mathbf{h}(\omega)$, so that $\chi(\omega)$ is a good estimate of $X(\omega)$. The performance of $\mathbf{h}(\omega)$ is then evaluated by means of beampattern, DF, and WNG, which are discussed in the next section.

B. Beampattern, DF, and WNG

The beampattern measures the array response to a plane wave from the θ direction. It is mathematically defined as [2]

$$\begin{aligned} \mathcal{B}[\mathbf{h}(\omega), \theta] &\triangleq \mathbf{d}_M^H(\omega, \cos\theta)\mathbf{h}(\omega) \\ &= \sum_{m=1}^{M} H_m(\omega) e^{\jmath(m-1)\omega\tau_0\cos\theta}. \end{aligned} \tag{5}$$

The DF quantifies the directional characteristic of a beamformer and is defined as the ratio between the magnitude squared beampattern in the desired direction and the averaged magnitude squared beampattern over the entire space [2], [27]. With a ULA, it is defined as

$$\begin{aligned} \mathcal{D}[\mathbf{h}(\omega)] &\triangleq \frac{|\mathcal{B}[\mathbf{h}(\omega), \theta_{\rm d}]|^2}{\frac{1}{2}\int_0^\pi |\mathcal{B}[\mathbf{h}(\omega), \theta]|^2 \sin\theta d\theta} \\ &= \frac{|\mathbf{h}^H(\omega)\mathbf{d}_M(\omega, \cos\theta_{\rm d})|^2}{\mathbf{h}^H(\omega)\mathbf{\Gamma}_M(\omega)\mathbf{h}(\omega)}, \end{aligned} \tag{6}$$

where

$$\mathbf{\Gamma}_M(\omega) \triangleq \frac{1}{2}\int_0^\pi \mathbf{d}_M(\omega, \cos\theta)\mathbf{d}_M^H(\omega, \cos\theta)\sin\theta d\theta \tag{7}$$

is the pseudo-coherence matrix of the spherically isotropic noise. It can be verified that the (i, j)th element of $\mathbf{\Gamma}_M(\omega)$ is

$$[\mathbf{\Gamma}_M(\omega)]_{i,j} = \frac{\sin[\omega\tau_0(i-j)]}{\omega\tau_0(i-j)}. \tag{8}$$

The maximum value of the DF is

$$\mathcal{D}_{\max}(\omega, \theta_{\rm d}) = \mathbf{d}_M^H(\omega, \theta_{\rm d})\mathbf{\Gamma}_M^{-1}(\omega)\mathbf{d}_M(\omega, \theta_{\rm d}), \tag{9}$$

which depends on ω, M, and $\theta_{\rm d}$. With a closely spaced ULA, $\mathcal{D}_{\max}(\omega, \theta_{\rm d})$ gives its maximum value at the endfire directions, which is equal to M^2 [29].

The WNG is used to measure the robustness of a beamformer with respect to the sensor self noise. It is defined as [2]

$$\mathcal{W}[\mathbf{h}(\omega)] \triangleq \frac{|\mathbf{h}^H(\omega)\mathbf{d}_M(\omega, \cos\theta_{\rm d})|^2}{\mathbf{h}^H(\omega)\mathbf{h}(\omega)}. \tag{10}$$

It is easy to check that the traditional delay-and-sum (DS) beamformer gives the maximum WNG, which is equal to M.

C. Objective of This Paper

With the signal model given in (2), the superdirective beamformer is typically derived from the following optimization problem with the assumption that the signal of interest is at the endfire direction, i.e., $\theta_{\mathrm{d}} = 0°$ [21]:

$$\min_{\mathbf{h}(\omega)} \mathbf{h}^H(\omega)\mathbf{\Gamma}_M(\omega)\mathbf{h}(\omega) \text{ subject to } \mathbf{h}^H(\omega)\mathbf{d}_M(\omega, 1) = 1. \tag{11}$$

The resulting beamformer can form a frequency-invariant beampattern [see Fig. 4(a.1)]. However, its WNG is very small at low frequencies [see the dashed gray line in Fig. 4(b.2)].

The objective of this paper is to develop robust superdirective beamformers that, on the one hand, have frequency-invariant beampatterns and, on the other hand, are insensitive to sensor self noise. The principle taken here is to reduce the order of the superdirective beamformer (with a smaller DF) while increasing the WNG.

III. Reduced-Order Superdirective Beamforming

A. Beamforming Structure

Following the analysis in [31], we can decompose the superdirective beamformer $\mathbf{h}(\omega)$ into the following form:

$$\mathbf{h}(\omega) = \mathbf{H}'(\omega)\mathbf{h}''(\omega), \tag{12}$$

where

$$\mathbf{H}'^H(\omega) = \begin{bmatrix} \mathbf{h}'^H(\omega) & & \mathbf{0}_{1\times(M''-1)} \\ 0 & \mathbf{h}'^H(\omega) & \mathbf{0}_{1\times(M''-2)} \\ \vdots & \ddots & \\ \mathbf{0}_{1\times(M''-1)} & & \mathbf{h}'^H(\omega) \end{bmatrix} \tag{13}$$

is a matrix of size $M'' \times M$,

$$\mathbf{h}'(\omega) = \left[H'_1(\omega)\ H'_2(\omega)\ \ldots\ H'_{M'}(\omega)\right]^T, \tag{14}$$

$$\mathbf{h}''(\omega) = \left[H''_1(\omega)\ H''_2(\omega)\ \ldots\ H''_{M''}(\omega)\right]^T, \tag{15}$$

and $M' + M'' - 1 = M$.

Substituting (12) into (5), we can rewrite the beampattern of $\mathbf{h}(\omega)$ as [31] (note this relationship holds only for ULAs; but it is not true, in general, for other array geometries)

$$\mathcal{B}[\mathbf{h}(\omega), \theta] = \mathcal{B}[\mathbf{h}'(\omega), \theta]\, \mathcal{B}[\mathbf{h}''(\omega), \theta], \tag{16}$$

where

$$\mathcal{B}[\mathbf{h}'(\omega), \theta] = \mathbf{d}^H_{M'}(\omega, \cos\theta)\mathbf{h}'(\omega), \tag{17}$$

$$\mathcal{B}[\mathbf{h}''(\omega), \theta] = \mathbf{d}^H_{M''}(\omega, \cos\theta)\mathbf{h}''(\omega). \tag{18}$$

According to (16), if we can make $\mathcal{B}[\mathbf{h}'(\omega), \theta]$ the same as the M'-order superdirective beampattern[1] and, at the same time, make $\mathcal{B}[\mathbf{h}''(\omega), \theta]$ flat over the entire space (i.e., omnidirectional), the global beampattern, $\mathcal{B}[\mathbf{h}(\omega), \theta]$, will be the M'-order superdirective beampattern and frequency invariant. Then, the redundancy of $\mathbf{h}''(\omega)$ can be exploited to improve the WNG.

Given the above decomposition, the objective of this paper is to design the sub-beamformer $\mathbf{h}'(\omega)$ so that it is a superdirective beamformer (we call it a reduced-order superdirective beamformer since $M' < M$) and the sub-beamformer $\mathbf{h}''(\omega)$ to improve the WNG.

[1] In principle, it could be any beampattern formed by other frequency invariant beamformers. An example is shown in Section V.

B. Design of $\mathbf{h}'(\omega)$

Since $\mathbf{h}'(\omega)$ is used to form an M'-order superdirective beampattern, it can be deduced from

$$\min_{\mathbf{h}'(\omega)} \mathbf{h}'^H(\omega)\mathbf{\Gamma}_{M'}(\omega)\mathbf{h}'(\omega) \text{ subject to } \mathbf{h}'^H(\omega)\mathbf{d}_{M'}(\omega, 1) = 1. \tag{19}$$

Solving (19), one can obtain

$$\mathbf{h}'_{\mathrm{S}}(\omega) = \frac{\mathbf{\Gamma}^{-1}_{M'}(\omega)\mathbf{d}_{M'}(\omega, 1)}{\mathbf{d}^H_{M'}(\omega, 1)\mathbf{\Gamma}^{-1}_{M'}(\omega)\mathbf{d}_{M'}(\omega, 1)}, \tag{20}$$

where the subscript S stands for "superdirective." Since the DF of this superdirective beamformer is closed to M'^2 [29], the value of M' can be easily determined in practice given the desired DF value.

C. Design of $\mathbf{h}''(\omega)$

Since $\mathbf{h}''(\omega)$ is used to improve the WNG, let us first write the WNG as a function of $\mathbf{h}''(\omega)$.

Substituting (12) into (10), we deduce the WNG of the overall beamformer as

$$\mathcal{W}[\mathbf{h}(\omega)] = \frac{\left|\mathbf{h}^H(\omega)\mathbf{d}_M(\omega, 1)\right|^2}{\mathbf{h}''^H(\omega)\mathbf{H}'^H(\omega)\mathbf{H}'(\omega)\mathbf{h}''(\omega)}. \tag{21}$$

According to (12) and the distortionless constraint in (19), we have

$$\begin{aligned} \mathbf{h}^H(\omega)\mathbf{d}_M(\omega, 1) &= \mathbf{h}''^H(\omega)\mathbf{H}'^H(\omega)\mathbf{d}_M(\omega, 1) \\ &= \mathbf{h}''^H(\omega)\mathbf{d}_{M''}(\omega, 1). \end{aligned} \tag{22}$$

Substituting (22) into (21), we get

$$\mathcal{W}[\mathbf{h}''(\omega)] = \frac{\left|\mathbf{h}''^H(\omega)\mathbf{d}_{M''}(\omega, 1)\right|^2}{\mathbf{h}''^H(\omega)\mathbf{H}'^H(\omega)\mathbf{H}'(\omega)\mathbf{h}''(\omega)}. \tag{23}$$

1) Maximum WNG Subbeamformer: From (23), it can be seen that the sub-beamformer that maximizes the WNG is

$$\mathbf{h}''_{\mathrm{MWNG}}(\omega) = \frac{\left[\mathbf{H}'^H(\omega)\mathbf{H}'(\omega)\right]^{-1}\mathbf{d}_{M''}(\omega, 1)}{\mathbf{d}^H_{M''}(\omega, 1)\left[\mathbf{H}'^H(\omega)\mathbf{H}'(\omega)\right]^{-1}\mathbf{d}_{M''}(\omega, 1)}, \tag{24}$$

where the subscript MWNG stands for "maximum WNG." While it maximizes the WNG, this sub-beamformer changes the global beampattern, particularly at high frequencies, making the beampattern frequency dependent.

2) Maximum Flatness Subbeamformer: According to (5), making $\mathcal{B}[\mathbf{h}''(\omega), \theta]$ constant over the entire space is equivalent to making it independent of $\cos\theta$, i.e.,

$$\frac{1}{2}\int_{-1}^{1}\left|\frac{\partial}{\partial\cos\theta}\mathcal{B}[\mathbf{h}''(\omega), \theta]\right|^2 d\cos\theta = 0. \tag{25}$$

Substituting (18) into (25), we deduce that

$$\mathbf{h}''^H(\omega)\mathbf{\Upsilon}(\omega)\mathbf{h}''(\omega) = 0, \tag{26}$$

where

$$\boldsymbol{\Upsilon}(\omega) = (\omega\tau_0)^2 \boldsymbol{\Sigma}\boldsymbol{\Gamma}_{M''}(\omega)\boldsymbol{\Sigma}^H, \tag{27}$$

$$\boldsymbol{\Sigma} \stackrel{\triangle}{=} \text{diag}\left(0,\ 1,\ 2,\ \ldots,\ M''-1\right). \tag{28}$$

Since $\boldsymbol{\Gamma}_{M''}(\omega)$ is positive definite, we have

$$\text{rank}\left[\boldsymbol{\Upsilon}(\omega)\right] = \text{rank}\left(\boldsymbol{\Sigma}\right) = M''-1, \tag{29}$$

which means that the dimension of the nullspace of $\boldsymbol{\Upsilon}(\omega)$ is equal to one. It is easy to verify that the eigenvector corresponding to the zero eigenvalue is

$$\mathbf{i}_1 = \begin{bmatrix} 1 & 0 & \cdots & 0 \end{bmatrix}^T. \tag{30}$$

Therefore, the maximum flatness filter is proportional to $\mathbf{i}_1$. By considering the distortionless constraint, i.e., $\mathbf{h}''^H(\omega)\mathbf{d}_{M''}(\omega,1) = 1$, the maximum flatness filter is

$$\mathbf{h}''_{\text{MF}}(\omega) = \mathbf{i}_1, \tag{31}$$

where the subscript MF stands for "maximum flatness." There is no redundancy left for improving the WNG. Substituting (20) and (31) into (12), the resulting global filter is just the M'-element ULA superdirective beamformer.

3) Flatness-Constrained Subbeamformer: Now, we consider relaxing the maximum flatness beampattern constraint given in (26). One way to relax (26) is to constrain the term $\mathbf{h}''^H(\omega)\boldsymbol{\Upsilon}(\omega)\mathbf{h}''(\omega)$ to be smaller than a small positive number instead of being equal to zero. As a result, the optimization problem for $\mathbf{h}''(\omega)$ can be expressed as

$$\min_{\mathbf{h}''(\omega)} \mathbf{h}''^H(\omega)\mathbf{H}'^H(\omega)\mathbf{H}'(\omega)\mathbf{h}''(\omega)$$
$$\text{subject to } \mathbf{h}''^H(\omega)\mathbf{d}_{M''}(\omega,1) = 1$$
$$\text{and } \mathbf{h}''^H(\omega)\boldsymbol{\Upsilon}(\omega)\mathbf{h}''(\omega) \le \gamma, \tag{32}$$

where γ is a small positive number. It is worth mentioning that one could use a convex optimization algorithm to directly solve the above problem [30]. However, it is more efficient to calculate the optimum beamformer iteratively. The solution of (32) can be expressed as

$$\mathbf{h}''_{\text{FC},\gamma}(\omega) = \frac{\left[\mathbf{H}'^H(\omega)\mathbf{H}'(\omega) + \epsilon_\gamma(\omega)\boldsymbol{\Upsilon}(\omega)\right]^{-1}\mathbf{d}_{M''}(\omega,1)}{\mathbf{d}^H_{M''}(\omega,1)\left[\mathbf{H}'^H(\omega)\mathbf{H}'(\omega) + \epsilon_\gamma(\omega)\boldsymbol{\Upsilon}(\omega)\right]^{-1}\mathbf{d}_{M''}(\omega,1)}, \tag{33}$$

where the subscript FC stands for "flatness constrained" and $\epsilon_\gamma(\omega) \ge 0$ controls the tradeoff between the WNG and the beampattern flatness. It can be verified that $\mathbf{h}''_{\text{FC},\gamma}(\omega)$ is equal to $\mathbf{h}''_{\text{MWNG}}(\omega)$ if $\gamma = +\infty$ [i.e., $\epsilon_\gamma(\omega) = 0$] and $\mathbf{h}''_{\text{FC},\gamma}(\omega)$ degenerates to $\mathbf{h}''_{\text{MF}}(\omega)$ if $\gamma = 0$ [i.e., $\epsilon_\gamma(\omega) = \infty$].

With the generalized eigenvalue decomposition, $\mathbf{H}'^H(\omega)\mathbf{H}'(\omega)$ and $\boldsymbol{\Upsilon}(\omega)$ can be jointly diagonalized as

$$\mathbf{H}'^H(\omega)\mathbf{H}'(\omega) = \mathbf{Q}^{-H}(\omega)\mathbf{Q}^{-1}(\omega), \tag{34}$$

$$\boldsymbol{\Upsilon}(\omega) = \mathbf{Q}^{-H}(\omega)\boldsymbol{\Lambda}(\omega)\mathbf{Q}^{-1}(\omega), \tag{35}$$

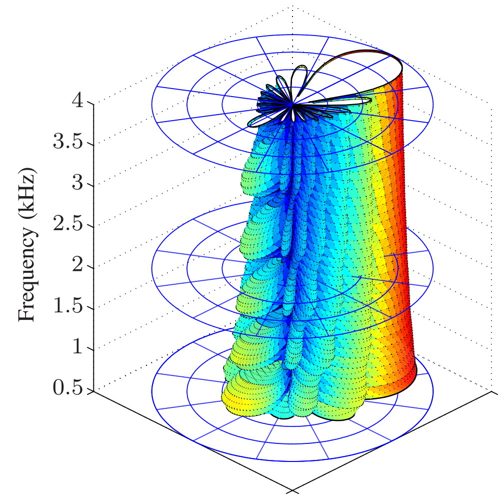

Fig. 2. Beampattern of the WNG-constrained superdirective beamformer as a function of frequency, where $M = 10$, $\delta = 2$ cm, and the minimum WNG is set to -20 dB.

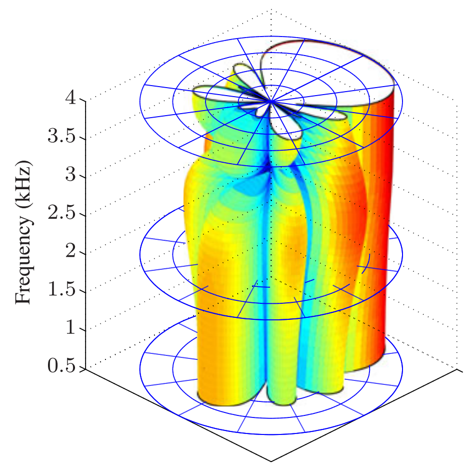

Fig. 3. Beampattern of the MWNG superdirective beamformer as a function of frequency, where $M = 10$, $M' = 4$, and $\delta = 2$ cm.

where

$$\mathbf{Q}(\omega) = \begin{bmatrix} \mathbf{q}_1(\omega) & \mathbf{q}_2(\omega) & \cdots & \mathbf{q}_{M''}(\omega) \end{bmatrix}, \tag{36}$$

$$\boldsymbol{\Lambda}(\omega) = \text{diag}\left[\lambda_1(\omega),\ \lambda_2(\omega),\ \ldots,\ \lambda_{M''}(\omega)\right], \tag{37}$$

with $\mathbf{q}_i(\omega)$ and $\lambda_i(\omega)$ [$\lambda_1(\omega) \ge \lambda_2(\omega) \ge \cdots \ge \lambda_{M''-1}(\omega) > \lambda_{M''}(\omega) = 0$], $i = 1, 2, \ldots, M''$, being the generalized eigenvectors and eigenvalues, respectively. Substituting (34) and (35) into (33), we can rewrite the beamformer as

$$\mathbf{h}''_{\text{FC},\gamma}(\omega) = \frac{\mathbf{Q}(\omega)\left[\mathbf{I} + \epsilon_\gamma(\omega)\boldsymbol{\Lambda}(\omega)\right]^{-1}\widetilde{\mathbf{d}}_{M''}(\omega,1)}{\widetilde{\mathbf{d}}^H_{M''}(\omega,1)\left[\mathbf{I} + \epsilon_\gamma(\omega)\boldsymbol{\Lambda}(\omega)\right]^{-1}\widetilde{\mathbf{d}}_{M''}(\omega,1)}, \tag{38}$$

where $\widetilde{\mathbf{d}}_{M''}(\omega,1) = \mathbf{Q}^H(\omega)\mathbf{d}_{M''}(\omega,1)$. It can be checked that the parameter $\epsilon_\gamma(\omega)$ satisfies the following (see Appendix A):

$$0 \le \epsilon_\gamma(\omega) \le \max\left[0,\ \frac{1}{\gamma} - \frac{1}{\lambda_1(\omega)}\right], \tag{39}$$

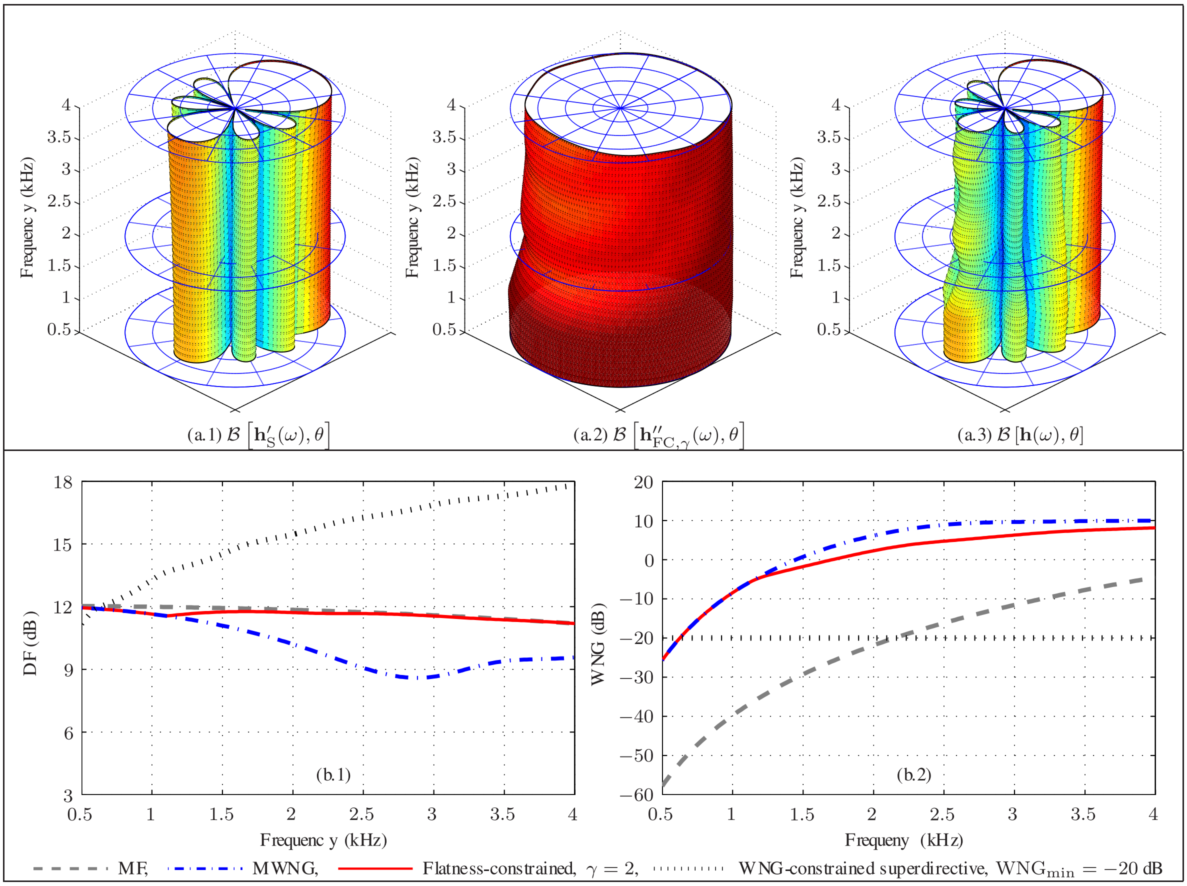

Fig. 4. Performance of the flatness-constrained beamformer with $M = 10$, $\delta = 2$ cm, $M' = 4$, and $\gamma = 2$. In (b.1) and (b.2), the DFs and WNGs of the WNG-constrained superdirective, MF, and MWNG beamformers are plotted for comparison.

and $\mathbf{h}''^{H}_{\rm FC,\gamma}(\omega)\boldsymbol{\Upsilon}(\omega)\mathbf{h}''_{\rm FC,\gamma}(\omega)$ is a monotonically decreasing function of $\epsilon_\gamma(\omega)$. Consequently, the optimal value of $\epsilon_\gamma(\omega)$ can be found with the well-known bisection method.

IV. Evaluation

In this section, we assess the proposed flatness-constrained beamformer in terms of beampattern, DF, and WNG. Note that we use both the terms sub-beamformer and beamformer. The former refers to either $\mathbf{h}'(\omega)$ or $\mathbf{h}''(\omega)$ while the latter refers to overall beamformer $\mathbf{h}(\omega)$.

We consider a ULA and want to achieve a DF of 12 dB. The frequency range that we are interested in is from 500 Hz to 4 kHz. Note that the WNG decreases dramatically at low frequencies, if signals under 500 Hz are of great interest, one can either use good microphone sensors with low self noise floor or use some other beamformers, e.g., delay-and-sum, that are robust to sensors' noise. The speed of sound in air is assumed to be 340 m/s. Given these conditions, the minimum wavelength is 8.5 cm. In the superdirective beamforming, the array interelement spacing should be much smaller than the half of minimum wavelength. As a result, we should have $\delta \ll 4.25$ cm. Let us choose the spacing as $\delta = 2$ cm in our simulation. Given the target DF of 12 dB (in other words, the desired DF value is equal to 16), M' should be equal to 4.

The filter $\mathbf{h}'_{\rm S}(\omega)$ and the matrix $\mathbf{H}'(\omega)$ are computed according to (20) and (13), respectively. The filter $\mathbf{h}''_{\rm FC,\gamma}(\omega)$ is computed according to (38), where the parameter $\epsilon_\gamma(\omega)$ is computed iteratively to satisfy the flatness constraint in (32). After determining $\mathbf{h}'_{\rm S}(\omega)$ and $\mathbf{h}''_{\rm FC,\gamma}(\omega)$, we compute the global beamformer, $\mathbf{h}(\omega)$, according to (12).

TABLE I
IFs for Different Beamformers, Where the Simulation Conditions are the Same as Those in Fig. 4

	MF	MWNG	Flatness-consstrained	WNG-constrained superdirective
IF (dB)	-29.7	-16.8	-25.1	-13.6

A. Results

In the first simulation, the number of sensors in the ULA is set to 10, i.e., $M = 10$, and the value of the parameter γ, which controls the flatness of the sub-beamformer, $\mathbf{h}''(\omega)$, is set to 2. For the purpose of comparison, we also present the performance of the well-known WNG-constrained superdirective beamformer, where the minimum WNG is set to be -20 dB.

According to the previous sections, the proposed flatness-constrained beamformer can be viewed as a tradeoff between the MF beamformer ($\gamma = 0$), whose beampattern is frequency invariant, and the MWNG beamformer ($\gamma = +\infty$), which has the largest WNG. Therefore, it is of importance to present the performance of both the MF and MWNG beamformers as well. The corresponding sub-beamformers are computed according to (20), (31), and (24), respectively.

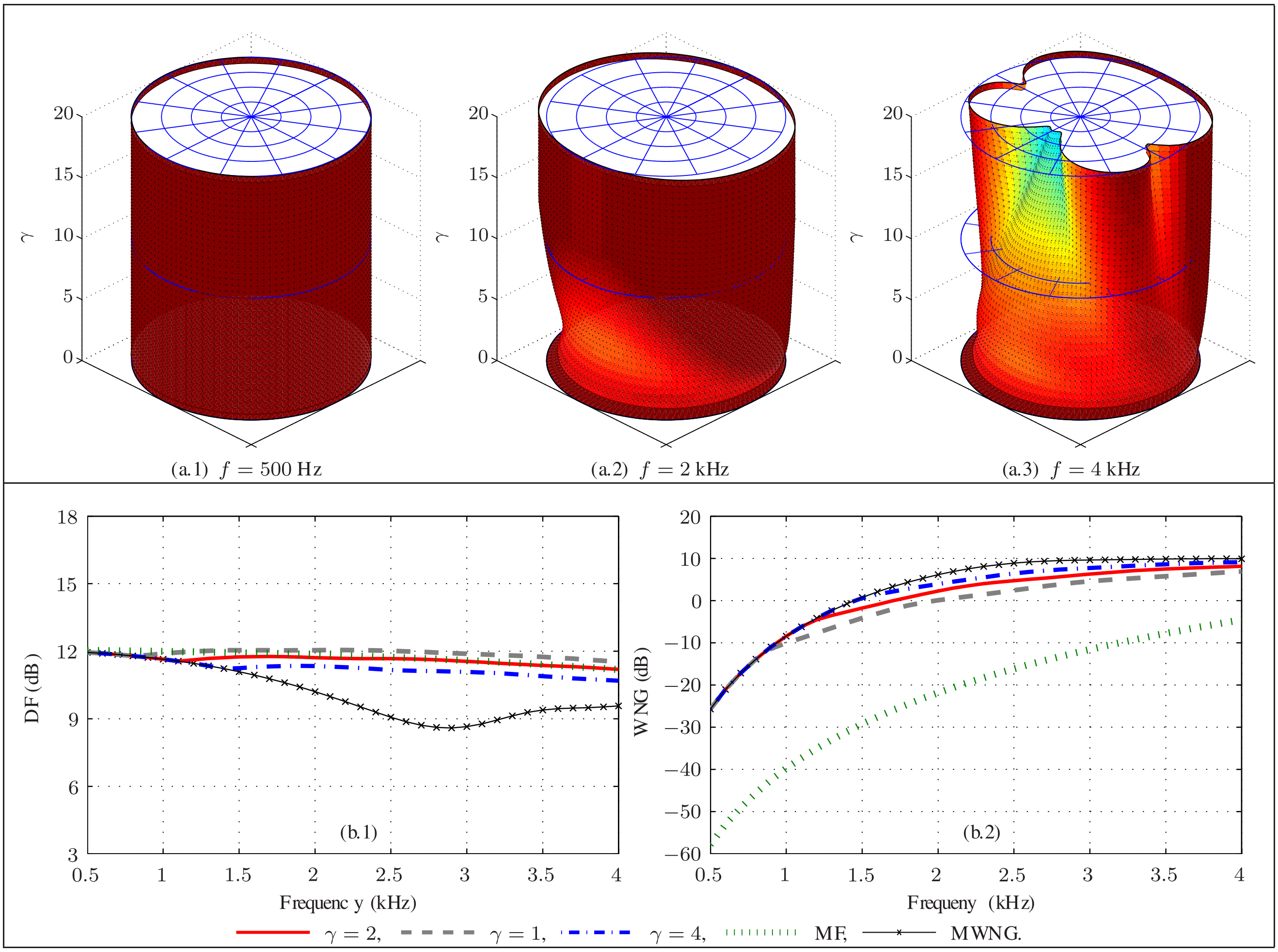

Fig. 5. Influence of the value of γ on the flatness-constrained beamformer with $M = 10$, $\delta = 2$ cm, and $M' = 4$. (a.1), (a.2), and (a.3) are beampatterns of the sub-beamformer $\mathbf{h}''_{\mathrm{FC},\gamma}(\omega)$ for three different frequencies, which are supposed to be flat. (b.1) and (b.2) are DFs and WNGs of the global beamformers.

1) Beampatterns: The beampatterns[2] of the WNG-constrained superdirective and MWNG beamformers are plotted in Figs. 2 and 3, respectively. As seen, they are both frequency dependent.

The beampatterns of the two sub-beamformers $\mathbf{h}'_{\mathrm{S}}(\omega)$ and $\mathbf{h}''_{\mathrm{FC},\gamma}(\omega)$, and the resulting flatness-constrained beamformer $\mathbf{h}(\omega)$ are plotted in Fig. 4(a.1), (a.2), (a.3). According to (16), the beampattern in (a.3) is the product of those in (a.1) and (a.2). As seen, the beampattern of $\mathbf{h}'_{\mathrm{S}}(\omega)$ is almost frequency invariant [see Fig. 4(a.1)]. The beampattern of $\mathbf{h}''_{\mathrm{FC},\gamma}(\omega)$ is quite flat over the entire space [see Fig. 4(a.2)]. As a result, the beampattern of the flatness-constrained beamformer is almost frequency invariant [see Fig. 4(a.3)].

To measure the degree of beampattern invariance, we define the invariance factor (IF) as

$$\mathrm{IF} \triangleq \frac{\frac{1}{P}\sum_{p=1}^{P}\sum_{q=1}^{Q}\left\{\left|\mathcal{B}\left[\mathbf{h}(\omega_p),\theta_q\right]\right| - \mathcal{M}\left(\theta_q\right)\right\}^2}{\sum_{q=1}^{Q}\mathcal{M}^2\left(\theta_q\right)}, \quad (40)$$

[2]In all the beampattern plots, the difference between the values of two adjacent circles in the same horizontal plane is 10 dB; the values of the outermost circle and the innermost dot are 0 dB and -40 dB, respectively.

where

$$\mathcal{M}\left(\theta_q\right) \triangleq \frac{1}{P}\sum_{p=1}^{P}\left|\mathcal{B}\left[\mathbf{h}(\omega_p),\theta_q\right]\right| \quad (41)$$

is the averaged magnitude of the beampattern over the frequency of interest, $\omega_p = 2\pi f_p$ is the discrete angular frequency with f_p being the temporal frequency, θ_q are the discrete angle, P and Q are the number of discrete frequencies and angles, respectively. In our simulation, f_p is from 500 Hz to 4 kHz with interval of 20 Hz; θ_q is from 0° to 180° with interval of 1°. The IFs, in dB, for different beamformers are shown in Table I. As we can see, the maximum flatness beamformer has the smallest IF, which is approximately -30 dB. The IF values of both the maximum WNG and WNG constrained superdirective beamformers are much larger than that of the maximum flatness beamformer, indicating that their beampatterns change significantly with frequency. In comparison, the IF value of the flatness-constrained beamformer is close to that of the maximum flatness beamformer, indicating that the flatness-constrained beamformer has almost frequency-invariant beampatterns.

2) DFs and WNGs: Fig. 4(b.1) and (b.2) plots the DFs and WNGs of the flatness-constrained, the MF (which is the same as the traditional non-robust superdirective), and the MWNG beamformers. As seen, the flatness-constrained beamformer

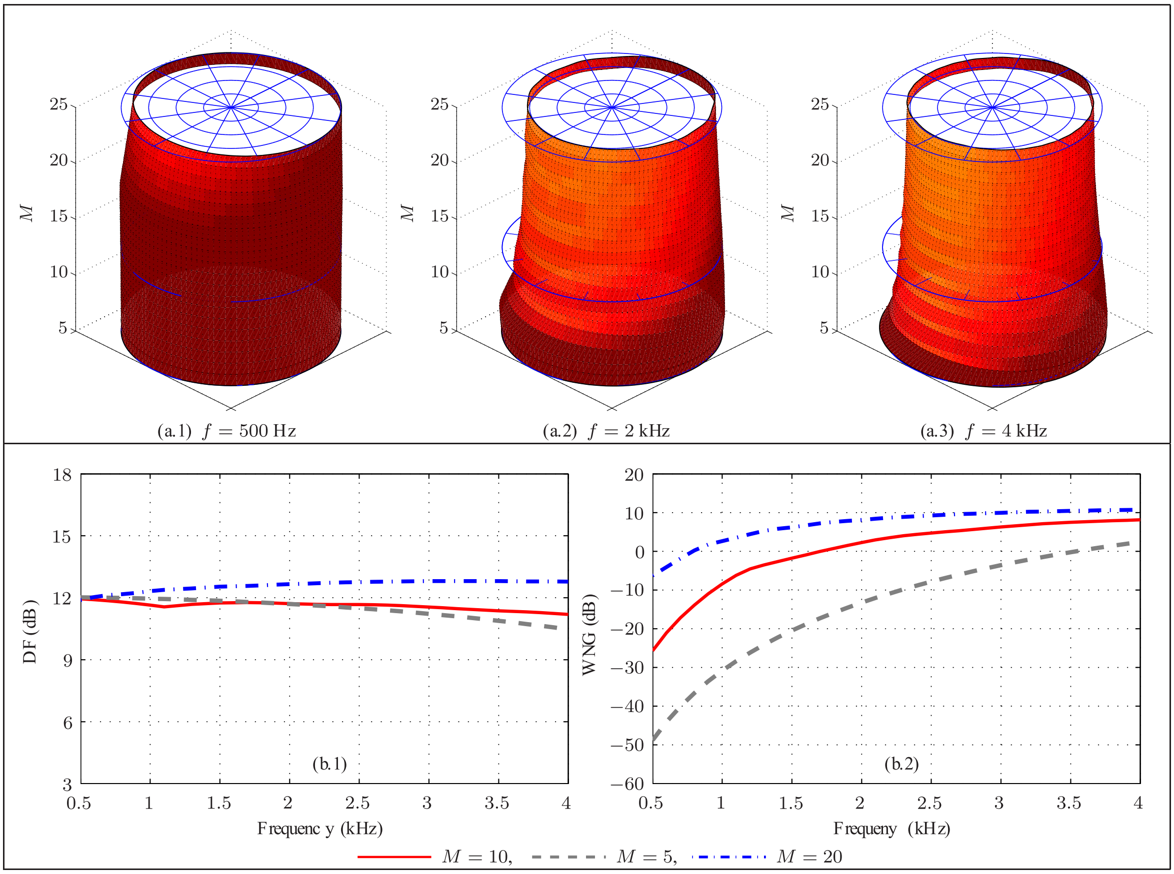

Fig. 6. Impact of the number of microphone sensors, M, on the performance of the flatness-constrained beamformer with $\gamma = 2$, $\delta = 2$ cm, and $M' = 4$. (a.1), (a.2), and (a.3) are beampatterns of the sub-beamformer $\mathbf{h}''_{\mathrm{FC},\gamma}(\omega)$ for three different frequencies, which are supposed to be flat. (b.1) and (b.2) are DFs and WNGs of the global beamformers.

with $\gamma = 2$ greatly improves the WNG as compared to the MF beamformer. In comparison with the MWNG beamformer, the flatness-constrained beamformer has a slightly smaller WNG, but its DF is much higher and almost frequency invariant.

B. Influence of γ, M, and δ on Performance

The performance of the flatness-constrained beamformer depends on the values of the parameters γ, M', M, and δ, where M' is determined by the desired DF value, and the other three parameters can be adjusted in the array design. In this section, we show the performance of the flatness-constrained beamformer with different values of γ, M, and δ.

1) Influence of γ: Fig. 5(a.1), (a.2), (a.3) plots the beampattern of the sub-beamformer $\mathbf{h}''_{\mathrm{FC},\gamma}(\omega)$ as a function of γ for three different frequencies. It can be seen that the beampattern flatness decreases as the value of γ increases. It approaches to that of the MWNG sub-beamformer, which forms flat beampattern at low frequencies and introduces extra nulls at high frequencies [31]. As the value of γ decreases, the beampattern becomes flatter and flatter till it is a constant over the entire space when γ equals zero.

The DFs and WNGs of the flatness-constrained beamformer with three different values of γ are plotted in Fig. 5(b.1) and (b.2). As seen, the DF and WNG of this beamformer get close to those of the MWNG beamformer as the value of γ increases. This confirms that the improvement in WNG is achieved by sacrificing the DF. With a smaller value of γ, the DF is more frequency invariant since the beampattern of $\mathbf{h}''_{\mathrm{FC},\gamma}(\omega)$ gets flatter; however, the WNG becomes smaller. Fortunately, at low frequencies where a large WNG improvement is needed, the beampattern of $\mathbf{h}''_{\mathrm{FC},\gamma}(\omega)$ is often flat. Therefore, the tradeoff between the WNG and the DF typically happens at higher frequencies. In practice, γ should be set as small as possible as long as the WNG improvement at low frequencies meets our requirement.

2) Influence of M: Fig. 6(a.1), (a.2), (a.3) plots the beampatterns of the sub-beamformer $\mathbf{h}''_{\mathrm{FC},\gamma}(\omega)$ as a function of M for three different frequencies. As seen, even with the same value of γ, the flatness of the beampattern changes slightly with M. More specifically, the beamformer has a higher DF value [see the blue curves in Fig. 6(b.1)] but the beampattern becomes less flat as more sensors are used. From this observation, a smaller value of γ should be used as M increases to ensure that the beampattern is frequency invariant in practice. The DFs and WNGs of the flatness-constrained beamformer with three different values of M are plotted in Fig. 6(b.1) and (b.2) (black curves). It can be seen that both the DF and the WNG increase with M.

3) Influence of δ: Fig. 7(a.1), (a.2), (a.3) plots the beampattern of the sub-beamformer $\mathbf{h}''_{\mathrm{FC},\gamma}(\omega)$ as a function of δ for three different frequencies. The DFs and WNGs of the flatness-constrained beamformer with three different values of δ are

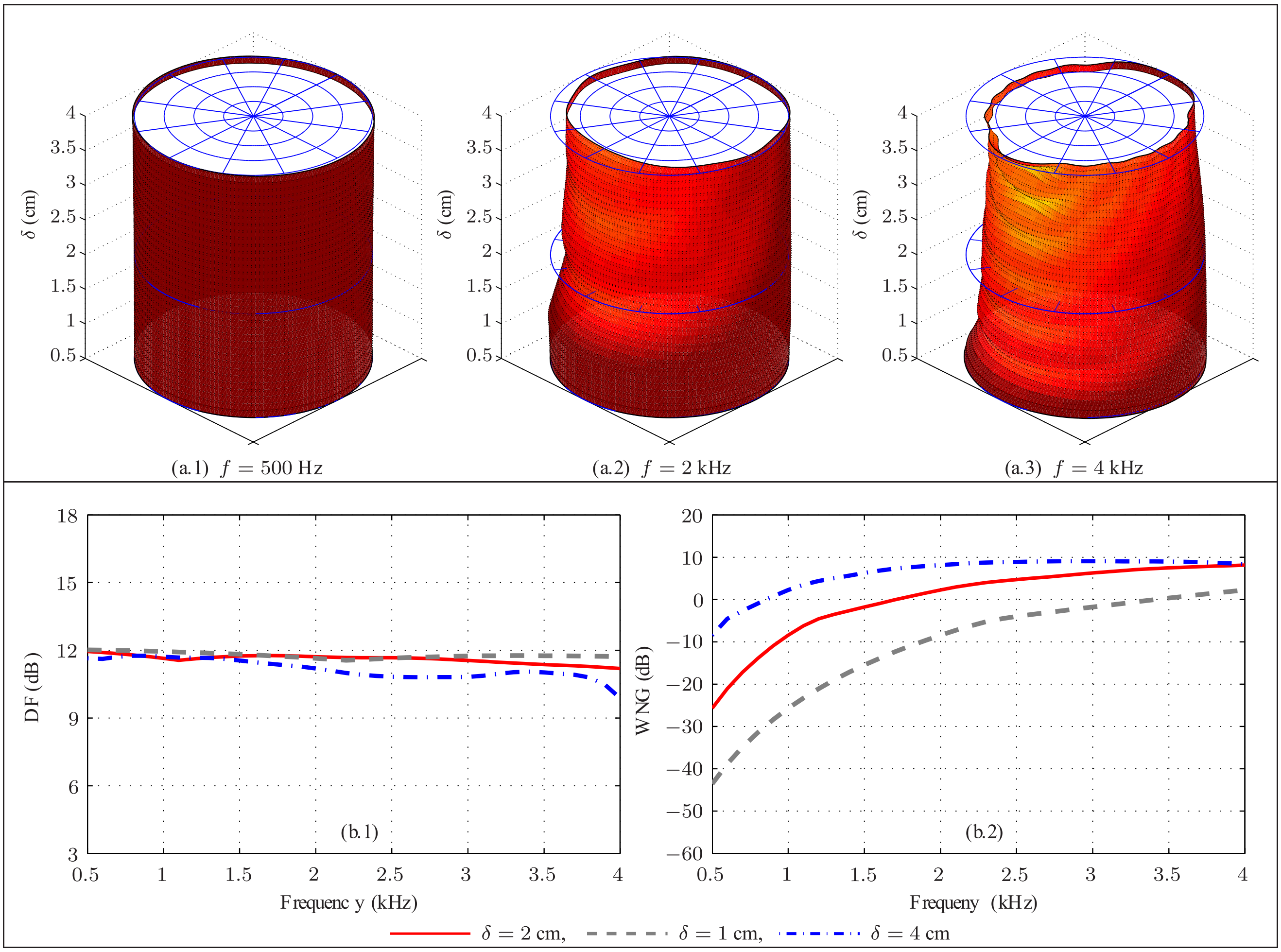

Fig. 7. Influence of the value of δ on the flatness-constrained beamformer with $\gamma = 2$, $M = 10$, and $M' = 4$. (a.1), (a.2), and (a.3) are beampatterns of the sub-beamformer $\mathbf{h}''_{\mathrm{FC},\gamma}(\omega)$ for three different frequencies, which are supposed to be flat. (b.1) and (b.2) are DFs and WNGs of the global flatness-constrained beamformers.

plotted in Fig. 7(b.1) and (b.2). Similar to the impact of increasing the number of sensors, increasing the value of δ can also improve the WNG. However, when δ approaches the half of the minimum wavelength ($\delta = 4.25$ cm in our case), the superdirective beamformer approaches the traditional DS beamformer,[3] which is no longer superdirective and both the DF and the frequency invariance of the beampattern are sacrificed. Therefore, with microphone arrays there is not much flexibility in changing the value of δ once the frequency range of interest is given. Empirically, $\delta = \lambda_{\min}/4$ is a good choice, where $\lambda_{\min}$ is the minimum wavelength given the frequency range of interest.

V. Extension to the Design of the Cardioid Beampattern

The principle of the flatness-constrained beamformer, though derived in the context of superdirective beamforming, can be extended to the design of other frequency-invariant beampatterns such as those in DMAs [2]. In this section, we show how it can be extended to the design of the cardioid beampattern, which is widely used in DMAs as the corresponding beamformer is optimal as far as the WNG is concerned [32].

The process of designing the flatness-constrained cardioid is the same as the design of the flatness-constrained superdirective beamformer shown in Section III. It consists of two steps: the first step is to find the sub-beamformer, $\mathbf{h}'(\omega)$, that can form the desired cardioid beampattern while the second step is to design the flatness-constrained sub-beamformer, $\mathbf{h}''(\omega)$. The second step is identical to that in Section III-C3. So, we only discuss how to design the sub-beamformer $\mathbf{h}'(\omega)$ for the cardioid.

According to [32], the M'-element traditional (non-robust) cardioid beamformer can be expressed as

$$\mathbf{h}'_{\mathrm{CD}}(\omega) = \frac{1}{\left(1 - e^{\jmath 2\omega\tau_0}\right)^N} \begin{bmatrix} 1 \\ -C_N^1 e^{\jmath\omega\tau_0} \\ \vdots \\ (-1)^n C_N^n e^{\jmath n\omega\tau_0} \\ \vdots \\ (-1)^N C_N^N e^{\jmath N\omega\tau_0} \end{bmatrix}, \tag{42}$$

[3]When the array interelement spacing equals half of the wavelength, i.e., $\omega\tau_0 = \pi$, the traditional superdirective beamformer degenerates to the DS beamformer.

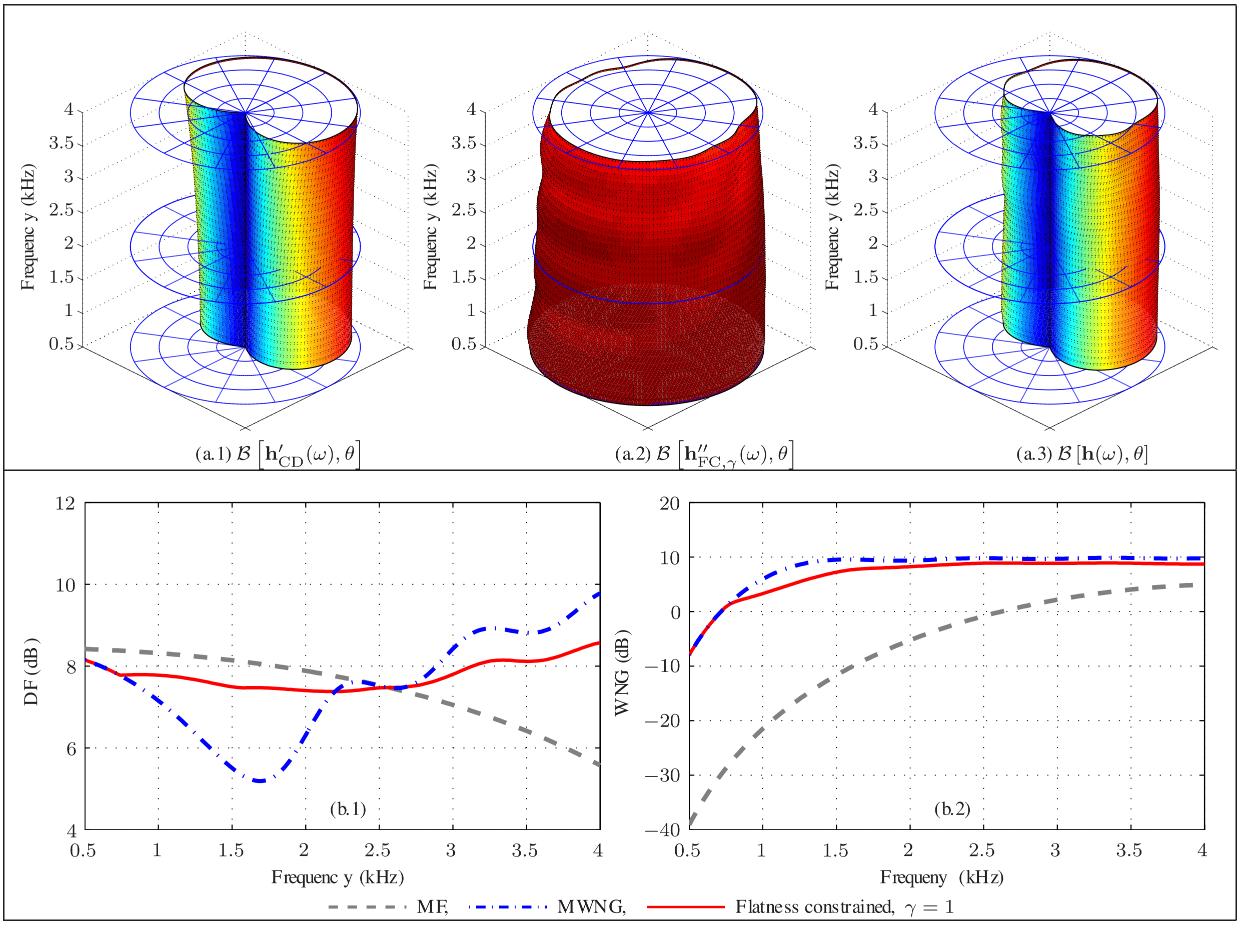

Fig. 8. Performance of the flatness-constrained cardioid beamformer, where $M = 10$, $M' = 4$, $\delta = 2$ cm, and $\gamma = 1$.

where CD stands for "cardioid," $n = 0, 1, \ldots, N$ with $N = M' - 1$, and $C_N^n = \frac{N!}{n!(N-n)!}$. In Appendix E, we show that the DF of this beamformer is approximately $2M' - 1$, which is larger than that of DS and many traditional additive beamformers.

Replacing $\mathbf{h}'_{\mathrm{S}}(\omega)$ by $\mathbf{h}'_{\mathrm{CD}}(\omega)$ in computing the flatness-constrained beamformer, we get the robust flatness-constrained cardioid beamformer. To evaluate the performance, we consider a ULA with 10 microphones. The value of M' is set to 4 and the value of γ is equal to 1. The corresponding beampatterns, DF, and WNG are plotted in Fig. 8.

VI. Conclusion

How to design robust and frequency-invariant beamformers is an important yet challenging problem. In this paper, we presented an approach to the design of robust superdirective beamformers. In this approach, the overall beamformer is divided into two sub-beamformers, which are convolved together: one sub-beamformer is formulated as a lower-order superdirective beamformer to achieve the desired DF and frequency-invariant beampattern and the other is optimized to improve the WNG with a flat spatial response over the entire space. Since it is the multiplication of beampatterns of two sub-beamformers, the beampattern of the overall superdirective beamformer is similar to (if not the same as) that of the lower-order superdirective sub-beamformer. A flatness-constrained superdirective beamformer is then derived, which can help improve the WNG while maintaining the overall beampattern approximately frequency invariant. The principle of the flatness-constrained superdirective beamformer can also be extended to other beamformers. As an example, we showed how to extend this principle to the design of the cardioid, which is widely used in differential beamforming.

Appendix A
Bounds of $\epsilon_\gamma(\omega)$

Let us first define the flatness function of the sub-beamformer $\mathbf{h}''_{\mathrm{FC},\gamma}(\omega)$ as

$$f\left[\epsilon_\gamma(\omega)\right] \triangleq \mathbf{h}''^H_{\mathrm{FC},\gamma}(\omega)\boldsymbol{\Upsilon}(\omega)\mathbf{h}''_{\mathrm{FC},\gamma}(\omega). \tag{43}$$

Substituting (35) and (38) into (43) gives

$$f\left[\epsilon_\gamma(\omega)\right] = \frac{\sum_{m=1}^{M''} \frac{\lambda_m(\omega)}{\left[1+\epsilon_\gamma(\omega)\lambda_m(\omega)\right]^2}\beta_m(\omega)}{\left[\sum_{m=1}^{M''} \frac{1}{1+\epsilon_\gamma(\omega)\lambda_m(\omega)}\beta_m(\omega)\right]^2}, \tag{44}$$

where

$$\beta_m(\omega) \triangleq \left|\mathbf{q}_m^H(\omega)\mathbf{d}_{M''}(\omega, 1)\right|^2. \tag{45}$$

Using the fact that $\mathbf{h}''_{\mathrm{FC},\gamma}(\omega)$ is also the solution of the following optimization problem:

$$\min_{\mathbf{h}(\omega)} \mathbf{h}''^H(\omega)\mathbf{H}'^H(\omega)\mathbf{H}'(\omega)\mathbf{h}''(\omega) + \epsilon_\gamma(\omega)\mathbf{h}''^H(\omega)\boldsymbol{\Upsilon}(\omega)\mathbf{h}''(\omega)$$
$$\text{subject to } \mathbf{h}''^H(\omega)\mathbf{d}_{M''}(\omega,1) = 1, \quad (46)$$

one can check that $f[\epsilon_\gamma(\omega)]$ is a monotonically decreasing function of $\epsilon_\gamma(\omega)$. Therefore, if we know the bounds of $\epsilon_\gamma(\omega)$, its value then can be determined with the bisection method.

Case 1: If the beampattern of the MWNG sub-beamformer is flat enough and no flatness constraint in (32) is needed, we then have

$$\epsilon_\gamma(\omega) = 0. \quad (47)$$

Case 2: If the flatness constraint is needed, the flatness function of the resulting beamformer is

$$f[\epsilon_\gamma(\omega)] = \gamma. \quad (48)$$

Therefore, we have

$$\gamma = \frac{\sum_{m=1}^{M''} \frac{\lambda_m(\omega)}{[1+\epsilon_\gamma(\omega)\lambda_m(\omega)]^2}\beta_m(\omega)}{\left[\sum_{m=1}^{M''} \frac{1}{1+\epsilon_\gamma(\omega)\lambda_m(\omega)}\beta_m(\omega)\right]^2} \quad (49)$$

$$\leq \frac{\frac{\lambda_1(\omega)}{1+\epsilon_\gamma(\omega)\lambda_1(\omega)}\sum_{m=1}^{M''} \frac{1}{1+\epsilon_\gamma(\omega)\lambda_m(\omega)}\beta_m(\omega)}{\left[\sum_{m=1}^{M''} \frac{1}{1+\epsilon_\gamma(\omega)\lambda_m(\omega)}\beta_m(\omega)\right]^2} \quad (50)$$

$$= \frac{\frac{\lambda_1(\omega)}{1+\epsilon_\gamma(\omega)\lambda_1(\omega)}}{\sum_{m=1}^{M''} \frac{1}{1+\epsilon_\gamma(\omega)\lambda_m(\omega)}\beta_m(\omega)} \quad (51)$$

$$\leq \frac{\frac{\lambda_1(\omega)}{1+\epsilon_\gamma(\omega)\lambda_1(\omega)}}{\frac{1}{1+\epsilon_\gamma(\omega)\lambda_{M''}(\omega)}\beta_{M''}(\omega)}, \quad (52)$$

where (49) is derived by substituting (44) into (48), the derivation from (49) to (50) is shown in Appendix C, the derivation from (50) to (51) is straightforward, and the derivation from (51) to (52) is shown in Appendix D. Considering that $\lambda_{M''}(\omega) = 0$ and $\beta_{M''}(\omega) = 1$ (see Appendix B), we deduce that

$$\gamma \leq \frac{\lambda_1(\omega)}{1+\epsilon_\gamma(\omega)\lambda_1(\omega)}, \quad (53)$$

which can be rewritten in the following form:

$$\epsilon_\gamma(\omega) \leq \frac{1}{\gamma} - \frac{1}{\lambda_1(\omega)}. \quad (54)$$

In conclusion, the bounds of $\epsilon_\gamma(\omega)$ are

$$0 \leq \epsilon_\gamma(\omega) \leq \max\left[0, \ \frac{1}{\gamma} - \frac{1}{\lambda_1(\omega)}\right]. \quad (55)$$

Appendix B
Proof of $\beta_{M''}(\omega) = 1$

According to (45), we have

$$\beta_{M''}(\omega) = \left|\mathbf{q}_{M''}^H(\omega)\mathbf{d}_{M''}(\omega,1)\right|^2, \quad (56)$$

where $\mathbf{q}_{M''}(\omega)$ is the eigenvector corresponding to the only zero eigenvalue of $\left[\mathbf{H}'^H(\omega)\mathbf{H}'(\omega)\right]^{-1}\boldsymbol{\Upsilon}(\omega)$. Recalling that the eigenvector corresponding to the only zero eigenvalue of $\boldsymbol{\Upsilon}(\omega)$ is $\mathbf{i}_1$, we have

$$\mathbf{q}_{M''}(\omega) = \mathbf{i}_1. \quad (57)$$

Substituting (57) into (56) gives

$$\beta_{M''}(\omega) = 1. \quad (58)$$

Appendix C
Derivation From (49) to (50)

Using the fact that $\lambda_1(\omega) \geq \lambda_m(\omega), \ \forall m \in \{1,2,\ldots,M''\}$, and $\epsilon_\gamma(\omega) \geq 0$, we have

$$\frac{\lambda_m(\omega)}{1+\epsilon_\gamma(\omega)\lambda_m(\omega)} \leq \frac{\lambda_1(\omega)}{1+\epsilon_\gamma(\omega)\lambda_1(\omega)}. \quad (59)$$

Multiplying both sides of (59) with $\frac{1}{1+\epsilon_\gamma(\omega)\lambda_m}$, we deduce that

$$\frac{\lambda_m(\omega)}{[1+\epsilon_\gamma(\omega)\lambda_m(\omega)]^2} \leq \frac{\lambda_1(\omega)}{1+\epsilon_\gamma(\omega)\lambda_1(\omega)} \times \frac{1}{1+\epsilon_\gamma(\omega)\lambda_m(\omega)}. \quad (60)$$

Since the $\beta_m(\omega)$'s are nonnegative by definition, we can deduce that

$$\frac{\lambda_m(\omega)}{[1+\epsilon_\gamma(\omega)\lambda_m(\omega)]^2}\beta_m(\omega) \leq \frac{\lambda_1(\omega)}{1+\epsilon_\gamma(\omega)\lambda_1(\omega)} \times \left[\frac{1}{1+\epsilon_\gamma(\omega)\lambda_m(\omega)}\beta_m(\omega)\right]. \quad (61)$$

Summing up both sides of (61) over m, we get

$$\sum_{m=1}^{M''} \frac{\lambda_m(\omega)}{[1+\epsilon_\gamma(\omega)\lambda_m(\omega)]^2}\beta_m(\omega) \leq \frac{\lambda_1(\omega)}{1+\epsilon_\gamma(\omega)\lambda_1(\omega)} \sum_{m=1}^{M''} \frac{1}{1+\epsilon_\gamma(\omega)\lambda_m(\omega)}\beta_m(\omega). \quad (62)$$

Substituting (62) into (49) gives (50).

Appendix D
Derivation From (51) to (52)

Considering that $\forall m \in \{1,2,\ldots,M''\}, \quad \lambda_m(\omega) \geq 0, \ \beta_m(\omega) \geq 0$, and $\epsilon_\lambda(\omega) \geq 0$, we have

$$\sum_{m=1}^{M''} \frac{1}{1+\epsilon_\gamma(\omega)\lambda_m(\omega)}\beta_m(\omega) \geq \frac{1}{1+\epsilon_\gamma(\omega)\lambda_{M''}(\omega)}\beta_{M''}(\omega). \quad (63)$$

Substituting (63) into (51) gives (52).

APPENDIX E
DF OF THE TRADITIONAL NTH-ORDER CARDIOID

Substituting (42) into (5), we deduce that the beampattern of the cardioid is

$$\begin{aligned}\mathcal{B}\left[\mathbf{h}'_{\mathrm{CD}}(\omega),\theta\right] &= \frac{1}{\left(1-e^{\jmath 2\omega\tau_0}\right)^N}\sum_{n=0}^{N}(-1)^n C_N^n e^{\jmath n\omega\tau_0(1+\cos\theta)} \\ &= \frac{1}{\left(1-e^{\jmath 2\omega\tau_0}\right)^N}\left[1-e^{\jmath\omega\tau_0(1+\cos\theta)}\right]^N. \end{aligned} \quad (64)$$

In the case that the array interelement spacing is much smaller than the wavelength, we have

$$e^{\jmath 2\omega\tau_0} \approx 1+\jmath 2\omega\tau_0, \quad (65)$$

$$e^{\jmath\omega\tau_0(1+\cos\theta)} \approx 1+\jmath\omega\tau_0(1+\cos\theta). \quad (66)$$

Substituting (65) and (66) into (64) gives

$$\mathcal{B}\left[\mathbf{h}'_{\mathrm{CD}}(\omega),\theta\right] \approx \frac{1}{2^N}\left(1+\cos\theta\right)^N. \quad (67)$$

Now, substituting (67) into (6), we obtain

$$\begin{aligned}\mathcal{D}\left[\mathbf{h}'_{\mathrm{CD}}(\omega)\right] &\approx \frac{2^{2N}}{\frac{1}{2}\int_0^{\pi}(1+\cos\theta)^{2N}\sin\theta d\theta} \\ &= \frac{2^{2N}}{\frac{1}{2}\int_{-1}^{1}(1+x)^{2N}dx} \\ &= 2N+1. \end{aligned} \quad (68)$$

Recalling that $N = M'-1$, we get

$$\mathcal{D}\left[\mathbf{h}'_{\mathrm{CD}}(\omega)\right] \approx 2M'-1. \quad (69)$$

REFERENCES

[1] D. B. Ward, R. C. Williamson, and R. A. Kennedy, “Broadband microphone arrays for speech acquisition,” *Acoust. Australia*, vol. 26, pp. 17–20, Apr. 1998.

[2] J. Benesty and J. Chen, *Study and Design of Differential Microphone Arrays*. Berlin, Germany: Springer-Verlag, 2012.

[3] J. Benesty, J. Chen, and I. Cohen, *Design of Circular Differential Microphone Arrays*. Switzerland: Springer-Verlag, 2015.

[4] G. W. Elko, “Differential microphone arrays,” in *Audio Signal Processing: For Next-Generation Multimedia Communication Systems*, Y. Huang and J. Benesty, Eds. New York, NY, USA: Springer, 2004, pp. 11–65.

[5] J. Chen, J. Benesty, and C. Pan, “On the design and implementation of linear differential microphone arrays,” *J. Acoust. Soc. Amer.*, vol. 136, pp. 3097–3113, Dec. 2014.

[6] J. Chen and J. Benesty, “A general approach to the design and implementation of linear differential microphone arrays,” in *Proc. Asia-Pacific Signal Inf. Process. Assoc. Annu. Summit Conf.*, 2013, pp. 1–7.

[7] H. Zhang, J. Chen, and J. Benesty, “Study of nonuniform linear differential microphone arrays with the minimum-norm filter,” *Appl. Acoust.*, vol. 98, pp. 62–69, Nov. 2015.

[8] L. Zhao, J. Benesty, and J. Chen, “Design of robust differential microphone arrays,” *IEEE/ACM Trans. Audio, Speech, Lang. Process.*, vol. 22, no. 10, pp. 1455–1466, Oct. 2014.

[9] L. Zhao, J. Benesty, and J. Chen, “Optimal design of directivity patterns for endfire linear microphone arrays,” in *Proc. IEEE Int. Conf. Acoust., Speech, Signal Process.*, 2015, pp. 295–299.

[10] C. Pan, J. Benesty, and J. Chen, “Design of robust differential microphone arrays with orthogonal polynomials,” *J. Acoust. Soc. Amer.*, vol. 138, pp. 1079–1089, 2015.

[11] G. W. Elko and J. Meyer, “Microphone arrays,” in *Springer Handbook of Speech Processing*, J. Benesty, M. M. Sondhi, and Y. Huang, Eds. Berlin, Germany: Springer-Verlag, 2008, pp. 1021–1041.

[12] T. Chou, “Frequency-independent beamformer with low response error,” in *Proc. IEEE Int. Conf. Acoust., Speech, Signal Process.*, vol. 5, 1995, pp. 2995–2998.

[13] F. Traverso, M. Crocco, and A. Trucco, “Design of frequency-invariant robust beam patterns by the oversteering of end-fire arrays,” *Signal Process.*, vol. 99, pp. 129–135, 2014.

[14] J. H. Doles III and F. D. Benedict, “Broad-band array design using the asymptotic theory of unequally spaced arrays,” *IEEE Trans. Antennas Propag.*, vol. 36, no. 1, pp. 27–33, Jan. 1988.

[15] D. B. Ward, R. A. Kennedy, and R. C. Williamson, “Theory and design of broadband sensor arrays with frequency invariant far-field beam patterns,” *J. Acoust. Soc. Amer.*, vol. 97, no. 2, pp. 1023–1034, Feb. 1995.

[16] C. P. Mathews and M. D. Zoltowski, “Eigenstructure techniques for 2-D angle estimation with uniform circular arrays,” *IEEE Trans. Signal Process.*, vol. 42, no. 9, pp. 2395–2407, Sep. 1994.

[17] J. Meyer, “Beamforming for a circular microphone array mounted on spherically shaped objects,” *J. Acoust. Soc. Amer.*, vol. 109, pp. 185–193, Jan. 2001.

[18] S. C. Chan and H. H. Chen, “Uniform concentric circular arrays with frequency-invariant characteristicsłtheory, design, adaptive beamforming and DOA estimation,” *IEEE Trans. Signal Process.*, vol. 55, no. 1, pp. 165–177, Jan. 2007.

[19] B. Rafaely, “Analysis and design of spherical microphone arrays,” *IEEE/ACM Trans. Audio, Speech, Lang. Process.*, vol. 13, no. 1, pp. 135–143, Jan. 2005.

[20] S. Yan, H. Sun, X. Ma, U. P. Svensson, and C. Hou, “Time-domain implementation of broadband beamformer in spherical harmonics domain,” *IEEE/ACM Trans. Audio, Speech, Lang. Process.*, vol. 19, no. 5, pp. 1221–1230, Jul. 2011.

[21] H. Cox, R. M. Zeskind, and T. Kooij, “Practical supergain,” *IEEE Trans. Acoust., Speech, Signal Process.*, vol. ASSP-34, no. 3, pp. 393–398, Jun. 1986.

[22] E. Mabande, A. Schad, and W. Kellermann, “Design of robust superdirective beamformers as a convex optimization problem,” in *Proc. IEEE Int. Conf. Acoust., Speech, Signal Process.*, 2009, pp. 77–80.

[23] S. Doclo and M. Moonen, “Superdirective beamforming robust against microphone mismatch,” *IEEE/ACM Trans. Audio, Speech, Lang. Process.*, vol. 15, no. 2, pp. 617–631, Feb. 2007.

[24] R. Berkun, I. Cohen, and J. Benesty, “Combined beamformers for robust broadband regularized superdirective beamforming,” *IEEE/ACM Trans. Audio, Speech, Lang. Process.*, vol. 23, no. 5, pp. 877–886, May 2015.

[25] C. Pan, J. Chen, and J. Benesty, “A multistage minimum variance distortionless response beamformer for noise reduction,” *J. Acoust. Soc. Amer.*, vol. 137, no. 3, pp. 1377–1388, Mar. 2015.

[26] M. Crocco and A. Trucco, “Design of robust superdirective arrays with a tunable tradeoff between directivity and frequency-invariance,” *IEEE Trans. Signal Process.*, vol. 59, no. 5, pp. 2169–2181, May 2011.

[27] L. L. Beranek, *Acoustics*. Woodbury, NY, USA: Acoustic Soc. Amer., 1986.

[28] J. Benesty, J. Chen, and Y. Huang, *Microphone Array Signal Processing*. Berlin, Germany: Springer-Verlag, 2008.

[29] A. I. Uzkov, “An approach to the problem of optimum directive antenna design,” *Comptes Rendus (Doklady) de l’Academie des Sciences de l’URSS*, vol. LIII, no. 1, pp. 35–38, 1946.

[30] M. Grant, S. Boyd, and Y. Ye, “CVX: Matlab software for disciplined convex programming, version 1.21 (2011),” 2010. [Online]. Available: cvxr. com/cvx/

[31] C. Pan, J. Chen, and J. Benesty, “Theoretical analysis of differential microphone array beamforming and an improved solution,” *IEEE/ACM Trans. Audio, Speech, Lang. Process.*, vol. 23, no. 11, pp. 2093–2105, Nov. 2015.

[32] C. Pan, J. Benesty, and J. Chen, “Design of directivity patterns with a unique null of maximum multiplicity,” *IEEE/ACM Trans. Audio, Speech, Lang. Process.*, vol. 24, no. 2, pp. 226–235, Feb. 2016.

[33] R. N. Marshall and W. R. Harry, “A new microphone providing uniform directivity over an extended frequency range,” *J. Acoust. Soc. Amer.*, vol. 12, pp. 481–498, Apr. 1941.

Chao Pan (SM'13) was born in 1989. He received the Bachelor's degree in electronics and information engineering from the Northwestern Polytechnical University (NPU), Xi'an, China, in 2011. He is currently working toward the Ph.D. degree in information and communication engineering with the NPU and also a visiting Ph.D. student at INRS-EMT, University of Quebec, Montreal, QC, Canada. His research interests include speech enhancement, noise reduction, and microphone array signal processing for hands-free speech communications.

Jingdong Chen (M'99–SM'09) received the Ph.D. degree in pattern recognition and intelligence control from the Chinese Academy of Sciences, Beijing, China, in 1998.

From 1998 to 1999, he was with the ATR Interpreting Telecommunications Research Laboratories, Kyoto, Japan, where he conducted research on speech synthesis, speech analysis, as well as objective measurements for evaluating speech synthesis. He then joined the Griffith University, Brisbane, Australia, where he was engaged in research on robust speech recognition, and signal processing. From 2000 to 2001, he worked at the ATR Spoken Language Translation Research Laboratories on robust speech recognition and speech enhancement. From 2001 to 2009, he was a Member of Technical Staff at Bell Laboratories, Murray Hill, NJ, USA, working on acoustic signal processing for telecommunications. He subsequently joined WeVoice Inc., New Jersey, serving as the Chief Scientist. He is currently a Professor at the Northwestern Polytechnical University, Xi'an, China. His research interests include acoustic signal processing, adaptive signal processing, speech enhancement, adaptive noise/echo control, microphone array signal processing, signal separation, and speech communication.

Dr. Chen served as an Associate Editor of the IEEE TRANSACTIONS ON AUDIO, SPEECH, AND LANGUAGE PROCESSING from 2008 to 2014 and as a Technical Committee (TC) member of the IEEE Signal Processing Society (SPS) TC on Audio and Electroacoustics from 2007 to 2009. He is currently a Member of the IEEE SPS TC on Audio and Acoustic Signal Processing, and a Member of the editorial advisory board of the *Open Signal Processing Journal*. He was the Technical Program Chair of the IEEE TENCON 2013, a Technical Program Co-Chair of the IEEE WASPAA 2009, the IEEE ChinaSIP 2014, the IEEE ICSPCC 2014, and the IEEE ICSPCC 2015, and helped organize many other conferences. He co-authored the books *Design of Circular Differential Microphone Arrays* (Springer, 2015), *Study and Design of Differential Microphone Arrays* (Springer, 2013), *Speech Enhancement in the STFT Domain* (Springer, 2011), *Optimal Time-Domain Noise Reduction Filters: A Theoretical Study* (Springer, 2011), *Speech Enhancement in the Karhunen-Loève Expansion Domain* (Morgan&Claypool, 2011), *Noise Reduction in Speech Processing* (Springer, 2009), *Microphone Array Signal Processing* (Springer, 2008), and *Acoustic MIMO Signal Processing* (Springer, 2006).

Dr. Chen received the 2008 Best Paper Award from the IEEE Signal Processing Society (with Benesty, Huang, and Doclo), the Best Paper Award from the IEEE Workshop on Applications of Signal Processing to Audio and Acoustics in 2011 (with Benesty), the Bell Labs Role Model Teamwork Award twice, respectively, in 2009 and 2007, the NASA Tech Brief Award twice, respectively, in 2010 and 2009, the Young Author Best Paper Award from the 5th National Conference on Man-Machine Speech Communications in 1998. He also received the Japan Trust International Research Grant from the Japan Key Technology Center in 1998 and the "Distinguished Young Scientists Fund" from the National Natural Science Foundation of China in 2014.

Jacob Benesty was born in 1963. He received the Master's degree in microwaves from Pierre & Marie Curie University, Paris, France, and the Ph.D. degree in control and signal processing from Orsay University, Orsay, France, in 1987 and 1991, respectively. From November 1989 to April 1991, during his Ph.D., he worked on adaptive filters and fast algorithms at the Centre National d'Etudes des Telecomunications, Paris, France. From January 1994 to July 1995, he worked at the Telecom Paris University on multichannel adaptive filters and acoustic echo cancellation. From October 1995 to May 2003, he was first a Consultant and then a Member of the Technical Staff at Bell Laboratories, Murray Hill, NJ, USA. In May 2003, he joined the University of Quebec, INRS-EMT, in Montreal, QC, Canada, as a Professor. He is also a Visiting Professor at the Technion, in Haifa, Israel, an Adjunct Professor at Aalborg University, in Denmark, and a Guest Professor at the Northwestern Polytechnical University, Xi'an, China. His research interests include signal processing, acoustic signal processing, and multimedia communications. He is the Inventor of many important technologies. In particular, he was the Lead Researcher at Bell Labs who conceived and designed the world-first real-time hands-free full-duplex stereophonic teleconferencing system. Also, he conceived and designed the world-first PC-based multi-party hands-free full-duplex stereo conferencing system over IP networks.

He was the Co-chair of the 1999 International Workshop on Acoustic Echo and Noise Control and the General Co-chair of the 2009 IEEE Workshop on Applications of Signal Processing to Audio and Acoustics. He received the IEEE Signal Processing Society 2001 Best Paper Award, with Morgan and Sondhi. and the IEEE Signal Processing Society 2008 Best Paper Award, with Chen, Huang, and Doclo. He is also the Co-author of a paper for which Huang received the IEEE Signal Processing Society 2002 Young Author Best Paper Award. In 2010, he received the "Gheorghe Cartianu Award" from the Romanian Academy. In 2011, he received the Best Paper Award from the IEEE WASPAA for a paper that he co-authored with Chen.